Permeability dependence of seismic amplitudes

Steven R. Pride, Université de Rennes, France
Jerry M. Harris, Stanford University, California, U.S.
David L. Johnson, Schlumberger-Doll Research, Ridgefield, Connecticut, U.S.
Albena Mateeva, Colorado School of Mines, Golden, Colorado, U.S.
Kurt T. Nihei, Lawrence Berkeley National Laboratory, California, U.S.
Robert L. Nowack, Purdue University, West Lafayette, Indiana, U.S.
James W. Rector, University of California at Berkeley, California, U.S.
Hartmut Spetzler, University of Colorado, Boulder, U.S.
Rushan Wu, University of California at Santa Cruz, California, U.S.
Tokuo Yamomoto, University of Miami, Florida, U.S.
James G. Berryman, Lawrence Livermore National Laboratory, California, U.S.
Michael Fehler, Los Alamos National Laboratory, New Mexico, U.S.

Can permeability be determined from seismic data? This question has been around since Maurice Biot, working for Shell in the 1950s, introduced the idea that seismic waves induce fluid flow in saturated rocks due to fluid-pressure equilibration between the peaks and troughs of a compressional wave (or due to grain accelerations in the case of a shear wave). Biot (1956) established a frequency-dependent analytical relation between permeability and seismic attenuation. However, laboratory, sonic log, crosswell, VSP, and surface seismic have all demonstrated that Biot's predictions often greatly underestimate the measured levels of attenuation—dramatically so for the lower-frequency measurements.

Yet, if an unresolved link truly exists between seismic amplitudes and permeability, the potential benefit to the oil industry is enormous. For this reason, the Department of Energy (DOE) brought together 15 participants from industry, national laboratories, and universities to concentrate for two days on whether permeability information is conceivably contained in and retrievable from seismic data. The present article represents much of the workshop discussion (which took place 5-6 December 2001 in Berkeley, California), but is not strictly limited to it.

Not all connections between hydrological and seismic properties are considered. Three-dimensional seismic images and time-lapse seismic monitoring are routinely used by reservoir engineers in constructing and constraining their reservoir model. Such imaging applications of seismic surveys to hydrological modeling are not discussed. Furthermore, in fractured reservoirs it is reasonable to postulate that any locally determined seismic anisotropy defines a symmetry class for the geologic material that must also be satisfied by the permeability tensor. Neither are such material-symmetry constraints discussed.

The focus here is only on whether the permeability of the rocks through which seismic waves propagate directly influences the decay of the wave amplitudes with distance. Key to addressing this question is an up-to-date discussion of the likely attenuation mechanisms operating in the exploration seismic band (10-10^3 Hz). We conclude that it indeed seems likely that the permeability structure of a geologic material is involved in explaining the observed levels of attenuation in the seismic band.

Possible inversion strategies for actually obtaining such permeability information are briefly discussed. However, we begin with the field measurements themselves.

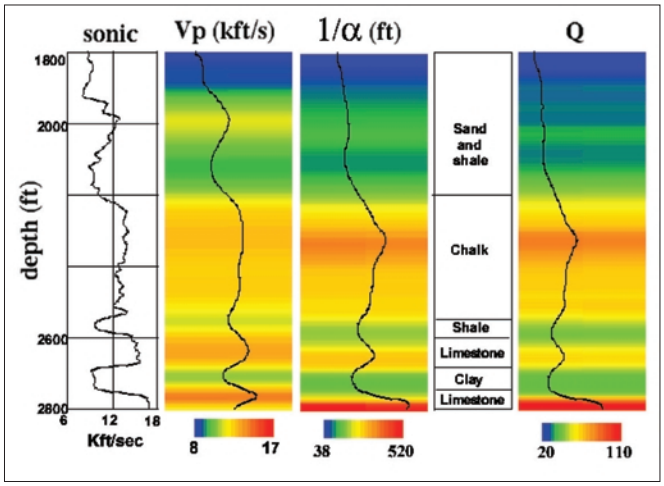

Figure 1. *P-wave velocity and attenuation tomograms (in color) calculated by Quan and Harris (1997) at BP's Devine test site.*

Measuring attenuation in the field. A multitude of methods have been used to determine attenuation from surface, VSP, or crosswell seismic data and we in no way attempt to be exhaustive in our coverage here.

In crosswell tomography, focus is most often placed on the waveform of the first arrival. The amplitude spectrum of the first arrival divided by the amplitude spectrum of the source is directly related to the average attenuation coefficient α (units of inverse length) along a raypath. This fact has been the basis for various tomographic strategies aimed at determining the attenuation structure within a given depth interval. Nowack and Matheney (1997) and Quan and Harris (1997) provide two effective approaches and references to earlier work.

For example, Quan and Harris determine P-wave velocity and attenuation tomograms using crosswell data from BP's Devine test site (Figure 1). The sedimentary sequence is known to have layer-cake structure at these depths and this fact is imposed on the inversion. The source spectrum has a center frequency of 1750 Hz and the medium is assumed to have constant Q over the range of frequencies involved; the quality factor Q is related to the attenuation coefficient α by $Q=\pi f/(\alpha v)$ where v is wave speed and f is frequency. The result from Figure 1 that we wish to highlight is the general level of attenuation present—namely, $10^{-2}<Q^{-1}<10^{-1}$ which is typical of

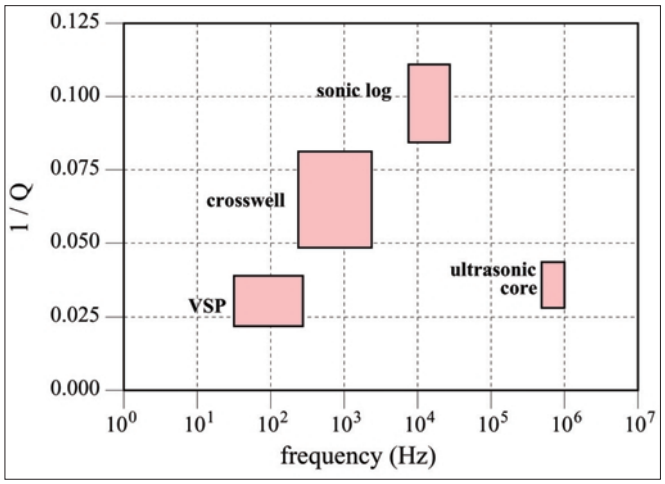

Figure 2. *Intrinsic P-wave attenuation 1/Q as determined by Sams et al. (1997) on rocks from the same geologic sequence. The number of Q estimates coming from different depth ranges that fall within each rectangle above are: 40 VSP, 69 crosswell, 854 sonic log, and 46 ultrasonic core measurements.*

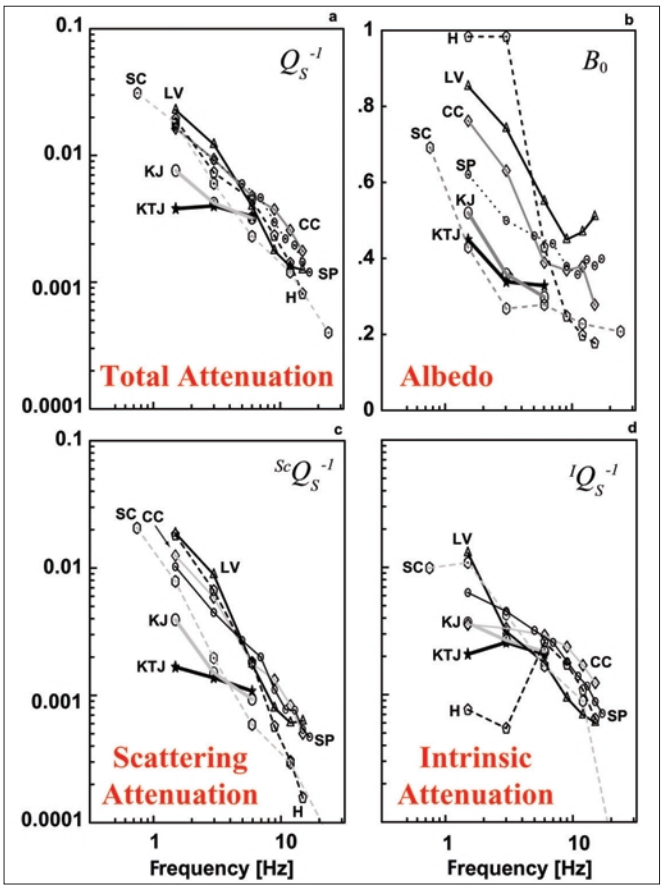

Figure 3. *S-wave attenuation determined from regional seismic data collected around the world (Sato and Fehler, 1998). The attenuation so determined corresponds to the average attenuation in each of the various crustal regions. The albedo is defined as $B_O = Q_{sc}^{-1}/Q_{total}^{-1}$. The various curves in each graph represent data from: KTJ-Kanto-Tokai, Japan; KJ=Kanto, Japan; LV=Long Valley, California; H=Hawaii; SC=Southern California; SP=Southern Spain; and CC=Central California.*

crosswell studies in sedimentary rocks at these and shallower depths.

An important series of experiments have been performed by Sams et al. (1997) at the Imperial College borehole test site in northeastern England. Four boreholes were drilled to a depth of a few hundred meters through a layered sequence of limestones, sandstones, siltstones, and mudstones. Cores were taken at many depths from one of the boreholes and ultrasonic measurements (300-900 kHz) of attenuation and velocity performed. Full-waveform sonic log (8-24 kHz), crosswell (200-2300 Hz), and VSP (30-280 Hz) experiments were also used to obtain the velocity and attenuation structure at the test site assuming constant Q for each measurement type and layer-cake structure. Figure 2 summarizes their results. The variance of the individual measurements within each rectangular box is due to the rock heterogeneity in the layered sequence. This is the only study we know of that has attempted attenuation measurements over such a broad range of frequencies for a single geologic sequence of rocks.

Sams et al. correct both their VSP and sonic log measurements to allow for scattering attenuation from the known layering present (to a first approximation, the horizontal crosswell measurements do not require such corrections). They determine that for the sonic-log measurement, the scattering attenuation is $1000/Q_{sc} = 5.5 \pm 2.3$, while the remaining intrinsic (= total - scattering) attenuation is $1000/Q_{in} = 96.5 \pm 4.6$ with the variance again due to the range of rock types present. For the VSP measurements, they determine a scattering attenuation of $1000/Q_{sc} = 8.3 \pm 1.4$ and an intrinsic attenuation of $1000/Q_{in} = 32 \pm 4.5$. Although there are uncertainties in estimating such scattering losses even for layer-cake structure, it may safely be concluded that for the sedimentary-rock sequence at the Imperial College test site, intrinsic attenuation dominates the scattering attenuation across the seismic band.

Determining and subtracting the scattering attenuation from the total apparent attenuation of seismic waves has been the subject of much research over the past 20 or so years—e.g., Wu and Aki (1988, 1989, 1990). The scattering from wavelength-scale and smaller heterogeneity has an absorption-like effect on transmitted seismic energy. Accordingly, the total apparent attenuation in transmission experiments is always greater than the intrinsic attenuation. This is not necessarily the case for reflection experiments because backscattering can sometimes enhance the apparent amplitude of the reflected energy. Techniques for separating intrinsic and scattering losses in surface seismic (reflection) data are not yet well developed (see Dasgupta and Clark, 1998, for a recent attempt). Accordingly, research on scattering attenuation has focused principally on transmission-dominated data such as earthquake, VSP, crosswell, sonic-log and laboratory data (though reflections can contribute significantly to both VSP and sonic data).

To account for scattering losses in sedimentary basins, the earth is often modeled as being finely layered. The properties of the fine layers are estimated from well logs and the scattering losses are most often estimated using the O'Doherty-Anstey (1971) transmission formula. If the scattering is due to random three-dimensional heterogeneity, radiative-transfer theory (see Sato and Fehler, 1998, for a review) is generally used. This theory demonstrates that the intensity of a seismic wave in a strongly scattering random material is controlled by a diffusion equation and not a wave equation when propagation distances are large compared to the distance between scatterers.

Sato and Fehler (1998) present a method called "multiple time-lapse window analysis" that uses a scalar radiative-transfer equation to fit the decay of the intensity of S-waves over different time windows in order to estimate the scattering contribution to the total attenuation of the wavefield. This method has been applied to both regional seismic data having propagation distances throughout the entire continental crust, and

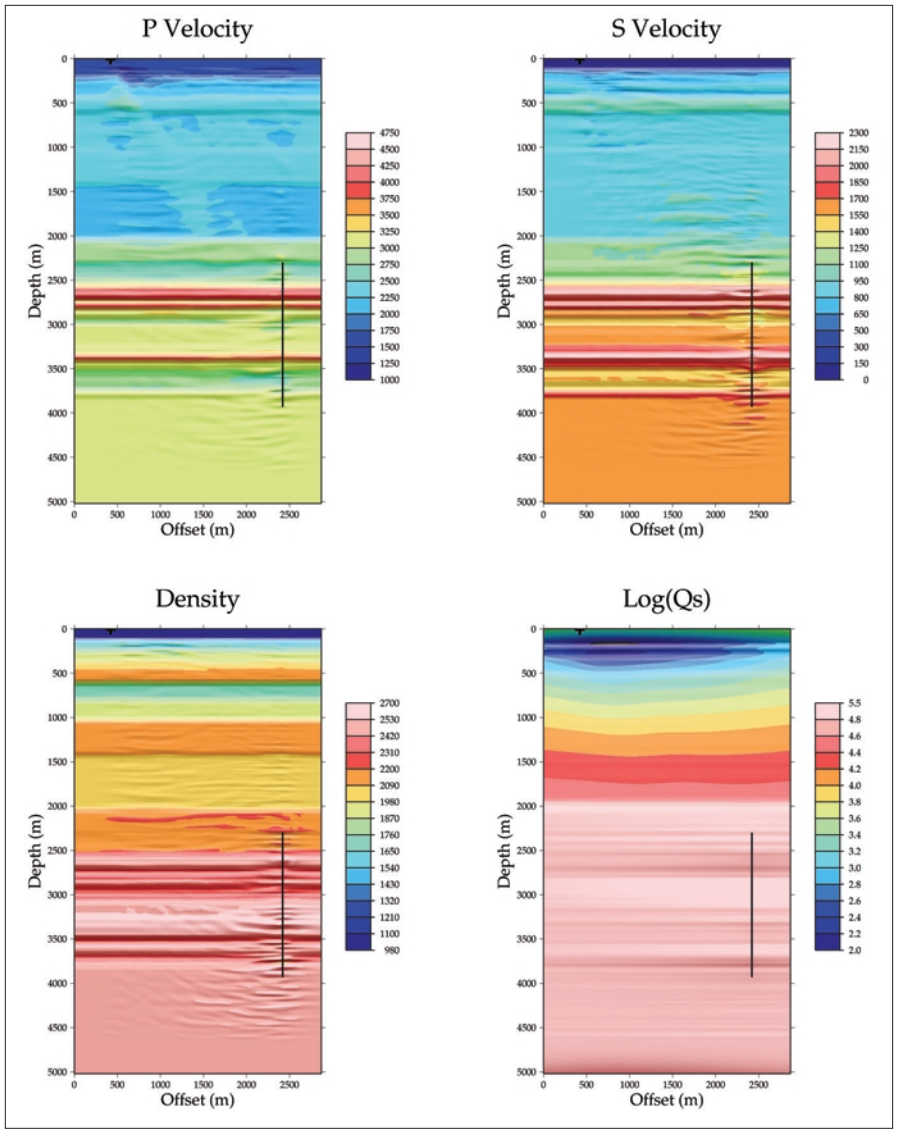

Figure 4. *The Charara et al. (1996) inversion results of an offset-vertical-seismic profile (OVSP) from the North Sea. The vertical line denotes the location of the three-component geophones. Only the Q_s associated with the shear modulus was modeled but this influences both the P-and S-wave propagation.*

to higher-frequency data collected over short distances. For example, Feustel et al. (1996) applied the method to 1 kHz data collected in mines. Figure 3 shows the Sato and Fehler analysis of regional earthquake data (propagation distances of 100-300 km) collected by various authors from various tectonic regimes throughout the world. It can be seen that at the scale of the entire crust, and for frequencies of 1-10 Hz, scattering and intrinsic attenuation contributes roughly equally to the total attenuation with the scattering fraction (the so-called "albedo") decreasing with increasing frequency. Interestingly, the scattering estimates of Sato and Fehler (1-10 Hz), Feustel et al. (1 kHz), and Sams et al. (100 Hz and 10 kHz) are all well fit (perhaps coincidentally) by the simple scaling law $Q^{-1}_{sc}/Q^{-1}_{total} \approx f^{-0.3}$.

The conclusion we wish to draw from these field measurements is that over a range of frequencies and therefore spatial scales, the intrinsic attenuation is not hopelessly smaller than the scattering attenuation; indeed, in these examples, it dominates the entire seismic band. Any direct relation between seismic amplitudes and permeability is necessarily due to the intrinsic attenuation and so these examples provide a positive first result.

Nonetheless, there can certainly be situations where intrinsic attenuation is simply not operative so that all attenuation is due to scattering. For example, Herkenhoff, Stefani, and Rector (results presented at a 2001 SEG regional conference in Baku, Azerbaijan) analyze deepwater offshore VSPs (frequencies near 100 Hz) and calculate the attenuation in intervals between 1300 and 2300 m below the seafloor. The rocks in this depth range are a stratified sequence of low-permeability tertiary shales. The measured interval attenuation falls within the range $3 \times 10^{-3} < Q^{-1} < 10^{-2}$ and these authors determine that scattering alone (O'Doherty-Anstey) can explain these relatively small values. The absence of intrinsic attenuation in this example is consistent with the idea that not much wave-induced flow can occur in such a deep shale sequence.

Ideally, the entire seismogram would be used to determine intrinsic attenuation and not just the waveform of the first arrival. One approach for doing so is that of Tarantola (1986) in which the difference between recorded and synthetic seismograms is iteratively minimized via conjugate-gradient updates of the material properties at each voxel of the earth (the inversion voxels have linear dimensions on the order of, or larger than, the central wavelength). The required Frechét derivatives defining how changes in a material property of a voxel affect the synthetic geophone data are best determined numerically; however, even with the recent advances in low-cost supercomputing, such direct calculations of the Frechét derivatives remain time prohibitive. Analytical approximations for these derivatives are normally employed, resulting in less-than-ideal updates. Furthermore, the success of a gradient search is controlled largely by the initial velocity model provided. The initial model must be built up from some combination of well-logs, moveout corrections, first-arrival tomography, and (ideally) Monte-Carlo searches using the entire seismic data set. Obtaining an accurate initial velocity structure is itself a nontrivial time-consuming effort.

Despite the enormous computational costs, such full-waveform inversion is attractive because scattering from the heterogeneity at scales larger than wavelengths is allowed for in the forward modeling, and the inversion is directly for the elastic moduli and intrinsic-attenuation material properties. Charara et al. (1996) use this approach to invert for seismic attenuation using offset-VSP data from a well in the North Sea (Figure 4). They do so assuming 3D wave propagation in a 2D earth structure. The residuals for this model (the difference betweeen the geophone data and synthetics) show that all the lower-frequency arrivals have been accounted for including difficult multiply reflected late arrivals. However, the highest frequency content of the data is not completely explained using this structure.

A practical near-term approach for using surface seismic data is to target certain regions or interfaces of interest, downward continue the prestack seismic wavefield to the targeted region, and perform AVO analysis on the local reflection. In order to obtain information about the attenuation in the targeted region, the downward continuation must preserve the relative amplitudes of the wavefield. It therefore must be performed using a wave equation with sufficient knowledge of the velocity structure that focusing/defocusing effects, interference of multiple arrivals, and diffraction/refraction effects are all reasonably allowed for in reconstructing the local reflection. Such "local inversion" of downward continued data has been the focus of much recent research including that by Wu and Chen (2002) and Chen and Wu (2002).

The physics of intrinsic attenuation in the seismic band. When a P-wave propagates through a fluid-saturated porous rock, it induces three types (or regimes) of fluid flow within an averaging volume. The averaging volume in this discussion may be thought of as the voxel or discretization element in a finite-difference forward model and corresponds to the finest resolution at which the seismic response is to be determined. The three regimes of wave-induced flow are defined by the distance over which the fluid pressure attempts to equilibrate by diffusion and will be called "macro," "micro," and "meso." The viscous flow in each case attenuates wave energy. No other loss mechanisms need be considered since, as will be seen, such wave-induced flow can explain the measured levels of intrinsic attenuation.

First, there is the macro or wavelength-scale equilibration between the peaks and troughs of a P-wave that Biot (1956) allowed for. At the scale of the averaging volume (which is much smaller than the wavelength), the wavelength-scale fluid-pressure gradient is equivalent to a uniform body force driving an incompressible flow across the volume. Because this body force continuously varies from one voxel to the next over a wavelength, there are fluid accumulations in the voxels and a fluid-pressure diffusion between the peaks and troughs of the wave. As for any diffusion process, the time necessary for the fluid-pressure differences to equilibrate goes as λ^2/D, where λ is the wavelength (the distance to be equilibrated) and D is the pore-pressure diffusivity. In a porous continuum, D is given by $D = Mk/\eta$, where k is the Darcy permeability, η the fluid viscosity, and M an elastic modulus called the "fluid-storage coefficient" that is well approximated as $M \approx K_f/\phi$ where ϕ is porosity and K_f the bulk modulus of the saturating fluid. The wavelength can be written $\lambda = \sqrt{H/\rho}/f$ where H is the P-wave elastic modulus, ρ the material density, and f the frequency (Hz). Maximum loss (as measured by $1/Q$) occurs when the wave period $1/f$ just equals the equilibration time λ^2/D and thus occurs at the relaxation frequency

$$f_c = \frac{H}{M}\frac{\eta}{\rho k}. \qquad (1)$$

Implicitly assumed in this order of magnitude estimate is that the material is uniform at the scale of each wavelength. Interestingly, the frequency f_c is of the same order of magnitude as that when viscous boundary layers first begin to develop in the pores of a rock (such boundary layers develop as the viscous "parabolic-profile" flow in the pores is replaced by inertia-dominated ideal "plug-profile" flow at sufficiently high frequencies). The onset of viscous-boundary layers formally occurs at the frequency $\eta/(\rho_f kF)$ where ρ_f is the fluid density and F is the electrical formation factor. Since $\rho M/H$ does not differ greatly from $\rho_f F$ for many rocks, fluid-pressure equilibration and viscous-boundary-layer development occur at about the same frequency. When $f >> f_c$, all loss in the Biot model is occurring in the viscous-boundary layers resulting in Q^{-1} falling off as $1/\sqrt{f}$; when $f << f_c$ (where Biot loss is not of seismological importance), Q^{-1} increases as fk/η.

Second, there is the micro equilibration that takes place at grain scales. Laboratory samples often have broken grain contacts and/or microcracks in the grains. Much of this damage occurs as a rock is brought from depth to the surface. Since diagenetic processes in a sedimentary basin tend to cement microcracks and grain contacts, it is uncertain whether in-situ rocks have significant numbers of open microcracks. Nonetheless, if such grain-scale damage is present, as it always is in laboratory rock samples at ambient pressures, the fluid-pressure response in the microcracks will be greater than in the principal porespace when the rock is compressed by a P-wave. Gary Mavko of Stanford University was the first to analyze the resulting flow from crack to pore which he called "squirt flow." Dvorkin et al. (1995) went on to establish a quantitative model for fully saturated rocks. In squirt flow, the time required for a microcrack of length R to equilibrate with a neighboring pore is R^2/D_h where the fluid-pressure diffusivity D_h in this case is that for a crack of aperture h and is given by $D_h \approx K_f h^2/\eta$. Equating the wave period $1/f$ to the equilibration time again determines the order-of-magnitude frequency at which the loss is maximum

$$f_c = \left(\frac{h}{R}\right)^2 \frac{K_f}{\eta}. \qquad (2)$$

This expression has several interesting features: (1) the dependence on fluid viscosity is just inverse to that in the Biot wavelength-scale equilibration; (2) there is no dependence on the permeability of the material (microcracks in the grains and/or broken grain contacts do not influence the permeability of a sandstone); and (3) since for water $K_f/\eta \approx 10^{12}$ Hz, the only way that squirt loss can peak in the seismic band is if the microcrack aspect ratios are quite small—e.g., $h/R < 10^{-4}$. However, as the aspect ratio decreases, so does the microcrack volume with the effect that the attenuation itself decreases with the aspect ratio. This idea is quantified momentarily.

Third, there is the flow at mesoscopic scales due to heterogeneity of the porous-continuum properties within each averaging volume. Wavelengths in the exploration band (10-10^3 Hz) range from hundreds of meters to meters so that the averaging volumes in seismic exploration have linear dimensions ranging from a few tens of centimeters (crosswell) to a few tens of meters (surface seismic). Earth materials within volumes of this size always have some degree of heterogeneity beyond that associated with the grains and pores. This could be due to, for example, interbedded shales and sands or joints/fractures embedded within a lower permeability sandstone. Even within an apparently homogeneous sandstone, there can be zones or pockets where the grains are less well cemented together (diagenesis is a transport-driven process and need not be spatially uniform). The physical effect of such heterogeneity is similar to squirt flow: where the framework of grains is relatively weak, the fluid pressure response will be greater than where it is relatively stiff. Fluid equilibration ensues but this time over some intermediate mesoscopic scale L as fixed by the heterogeneity within an averaging volume. The maximum loss associated with such flow again occurs when $1/f_c = L^2/D$ or

$$f_c = \frac{M}{L^2}\frac{k}{\eta} \approx \left(\frac{k}{\phi L^2}\right)\frac{K_f}{\eta}, \qquad (3)$$

where M, k, and ϕ are the storage coefficient, permeability, and porosity of the porous matrix material within which the softer material is embedded. The dependence of the relaxation frequency on the ratio k/η is just opposite to that in

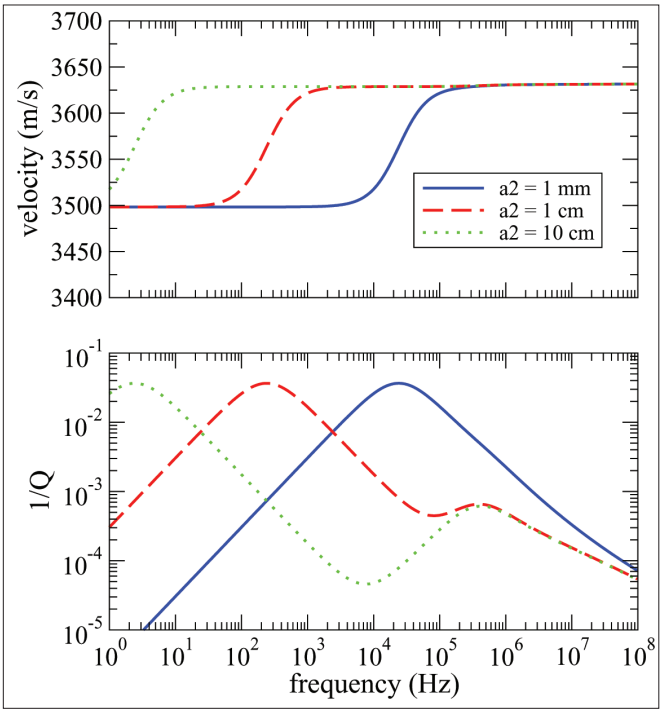

Figure 5. *The double-porosity mesoscopic flow model of Pride and Berryman (2003). The properties chosen correspond to small spherical pockets (having radius a_2) of a soft phase 2 material embedded within a stiffer consolidated sandstone-like material. The permeability of the host phase 1 is k=10 mD and the volume fraction occupied by phase 2 is a constant 1.5%. Results for wavelengths less than a_2 (e.g., $f > 100$ kHz when $a_2 = 1$ cm) are formally invalid for the mesoscopic part of the attenuation since the averaging volume upon which the theory is based must have a size greater than a_2 but less than wavelengths.*

Biot theory (again, this is simply due to the equilibration length in Biot theory being the frequency-dependent wavelength). This mesoscopic-loss mechanism can peak anywhere within the seismic band depending on the permeability of the material and the length scale L of the heterogeneity.

Pride and Berryman (2003) have quantified the mesoscopic-loss model by considering averaging volumes in which only two porosity types are present (a so-called double porosity model). Porous phase 1 is taken to be a relatively stiff host material, while phase 2 is taken to be a relatively soft and permeable embedded material (for example, zones where the cementing between the grains is less developed). Pride and Berryman determine analytical expressions for the frequency dependence of the poroelastic moduli in the presence of such mesoscopic-scale structure. Figure 5 shows typical results using values for phase 1 corresponding to a consolidated sandstone. In this example, the size a_2 of the inclusion is varied while the volume fraction occupied by phase 2 is fixed at a constant 1.5%. The small attenuation peak near 500 kHz is that associated with wavelength-scale equilibration (the Biot loss) while the main peak is that due to the mesoscopic heterogeneity. Figure 6 shows how 1/Q varies in the same model when only the permeability of the host phase is varied with $a_2 = 1$ cm. At any given frequency, Q is seen to be linearly proportional to permeability and thus quite sensitive to variations in permeability.

The levels of attenuation in these models are comparable to that actually measured in the field.

Another important source of mesoscopic heterogeneity is patchy saturation. In gas patches where the fluid incompressibility is quite small, a wave only induces a small change in the fluid pressure while in liquid patches where

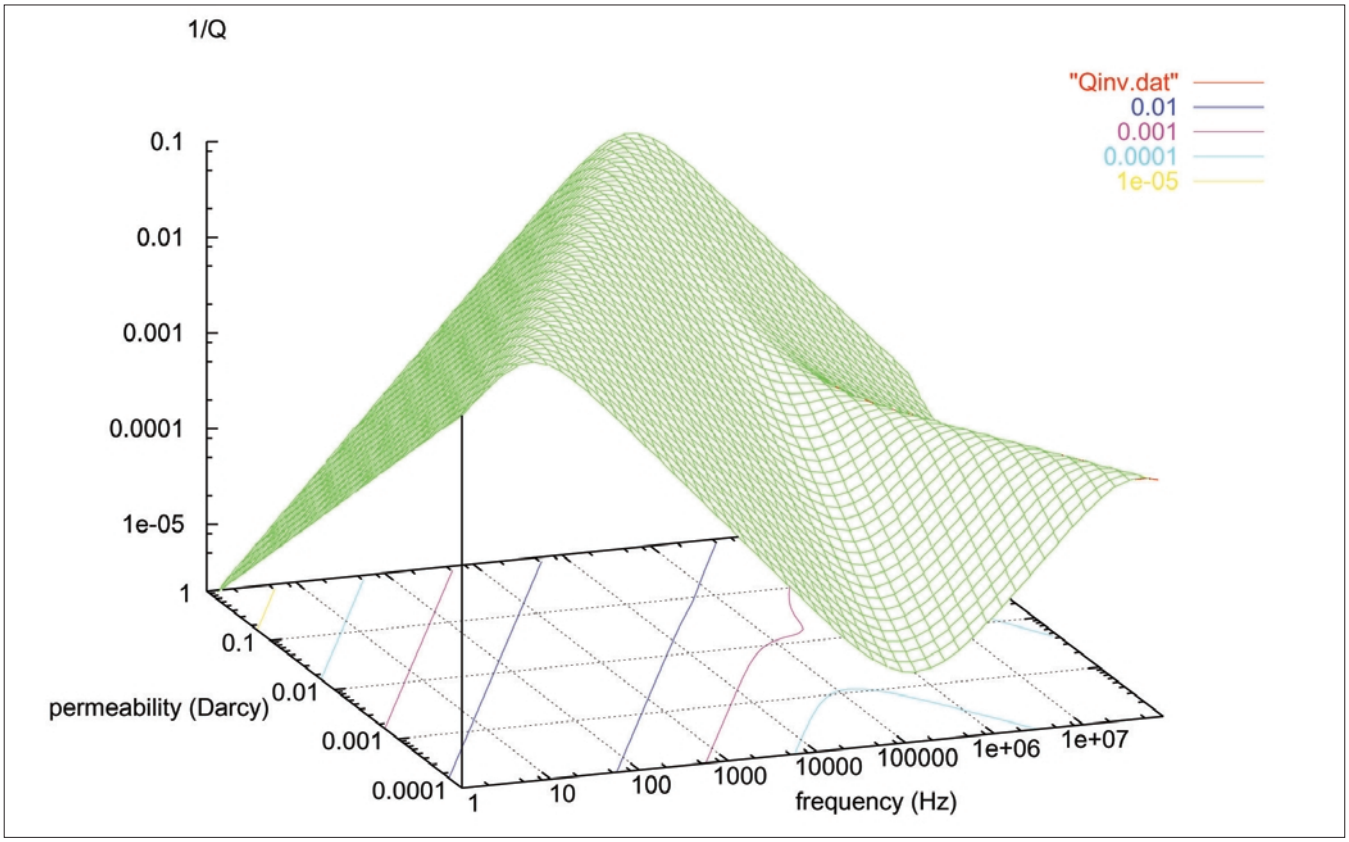

Figure 6. *The permeability and frequency dependence of the P-wave attenuation when mesoscopic flow is allowed for. The smaller ridge in the attenuation surface near 1 MHz corresponds to the Biot losses. The dominant ridge that has opposite permeability dependence is due to the mesoscopic flow. This example has the same fixed properties as that in Figure 5 and an inclusion dimension of $a_2 = 1$ cm.*

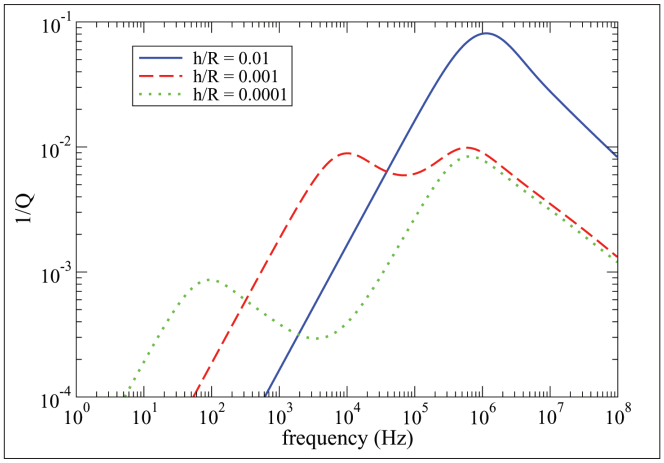

Figure 7. *The squirt-flow model when the drained bulk modulus of a porous grain is taken to be dependent on the aspect ratio h/R of the microcracks within it.*

the fluid incompressibility is relatively large, a large fluid pressure is induced. There is a subsequent fluid-pressure equilibration between the patches that attenuates wave energy. Johnson (2001) has provided a rigorous model of attenuation in such materials that is quite similar to the Pride and Berryman model discussed above. In general, Q^{-1} can be very large in the seismic band (exceeding 0.1) for such a patchy-saturation model with the peak in Q^{-1} again dependent on the permeability of the material and the effective patch sizes.

We underline that the general features of the mesoscopic-scale loss are similar whether the heterogeneity is in the fluid properties or in the elastic moduli of the framework of grains. In particular, the mesoscopic loss in either case increases as $Q^{-1} \alpha fk/\eta$ when $f << f_c$ which makes it quite distinct from the Q^{-1} & fk/η low-frequency increase in the Biot model.

Last, we consider whether the measured attenuation in the seismic band can be explained using the squirt mechanism with suitably chosen parameters. In the squirt model of Dvorkin et al., the grains of a porous material are themselves allowed to have porosity in the form of microcracks. The effect of each broken grain contact is taken to be equivalent to a microcrack in a grain. The number of such microcracks per grain is thus limited by the coordination number of the packing (the number of contacts per grain). The two key parameters of the squirt model are: (1) the aperture of the microcracks in the grains as normalized by the size of the grains (the aspect ratio h/R) that is controlling the time scale of equilibration, and (2) the effective drained bulk modulus of an isolated grain containing microcracks that is controlling the fluid-pressure differences between the grain porosity and bulk porosity. This effective drained grain modulus is necessarily a function of the aspect ratio of the microcracks, as effective-medium theory makes clear. As h/R is decreased, the drained grain modulus increases (in the limit that $h/R \rightarrow 0$, the drained grain modulus must approach the mineral modulus) so that the fluid-pressure difference between the cracks and pores is reduced along with the associated attenuation. Dvorkin et al. treated these two parameters as independent fitting constants and thus never commented about this relation. Figure 7 shows a typical result when the drained modulus of a grain is allowed to increase with decreasing aspect ratio. If the peak in squirt is driven down to the seismic band by making the aspect ratio sufficiently small, the peak loss is also driven down due to there being less fluid volume in the microcracks. In this figure, the peak to the right near 1 MHz again corresponds to the Biot loss associated with wavelength-scale equilibration.

From these results, we conclude that there is reason to believe that intrinsic attenuation in the seismic band is controlled by mesoscopic flow. And since such mesoscopic flow is sensitive to the permeability of the materials involved, there is indeed hope that permeability information is contained within seismic data.

Forward and inverse modeling. We now consider how to extract such permeability dependence from the seismic data. Standard thinking might be to use some viscoelastic forward model (for example constant Q_p and Q_s associated with the volumetric and shear response), and to invert the data for Q_p, Q_s, and the velocities at each inversion voxel. Given the Q_p, Q_s, and velocities, the idea might then be to use a "rock physics" relation that translates such seismic measures into permeability estimates.

Such a "standard" approach is not without hope if we free the limitation to constant Q models (as Figure 2 suggests we should) and attempt broad-band measurements of $Q(\omega)$ from, say, 100 Hz to 10 kHz in crosswell studies. The Q_p, Q_s, V_P, and V_S variations in space and frequency can then be interpreted using the mesoscopic-flow model in order to place constraints on the permeability.

For example, the mesoscopic model suggests that the presence of pockets or layers of a softer material embedded within an inversion voxel is potentially responsible for significant mesoscopic flow due to the large local fluid-pressure gradients created. A priori, one might expect for Q_p^{-1} to go up in such a voxel while certainly V_P drops relative to a voxel that has little or no soft inclusions. However, if the frequency is such that the dimensionless grouping of properties $K_f k/(L^2 \phi \eta f)$ (that equals 1 when mesoscopic loss is maximum) is either much less or much greater than one, then one could have a small Q_p^{-1} even though V_P is anomalously small (we would then be on either side of the peak attenuation in Figures 5 and/or 6). By tracking how Q_p changes with frequency over a broadband measurement, estimates of the ratio $k/\phi L^2$ could be obtained, and by tracking how the velocities change in space, information about L might conceivably be inferred.

We will not detail here an algorithm for performing such an analysis, but it is certainly reasonable to think that knowledge of Q_p, Q_s, V_P, and V_S in space and frequency, when coupled with the mesoscopic-flow model, could provide constraints on permeability. We emphasize that the permeability being inverted for is that of the matrix material within which the mesoscopic heterogeneity is embedded in each inversion voxel. This permeability is formally distinct from the overall hydrological permeability of the voxel defined by applying pressure drops across the voxel and measuring the total fluid flux into and out of the voxel. The distinction between these two permeabilities is related to how the mesoscopic heterogeneity is connected across each inversion voxel.

An alternative inversion strategy is to build the proper permeability and frequency dependence directly into the seismic forward model. If computer power were not a limiting factor (unfortunately, it is), the following scheme based on using Biot theory with fine discretization would be reasonable.

First the earth is discretized into "inversion voxels" that have linear dimensions on the order of (or larger than) the central wavelength of the experiment. As discussed earlier, such an inversion voxel might be on the order of 1 m^3 in a

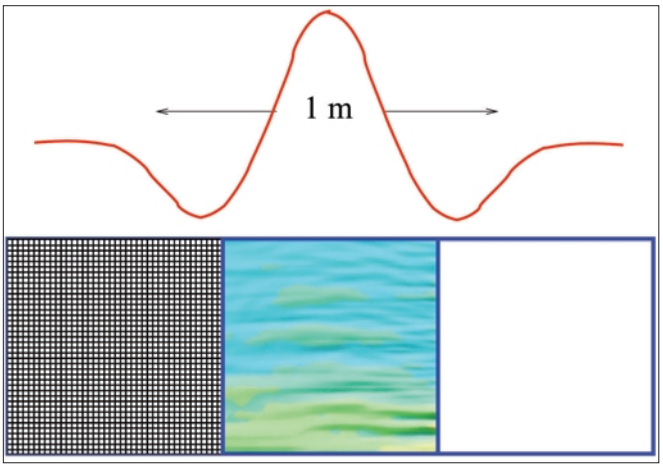

Figure 8. The blue grid corresponds to the inversion voxels while the fine black grid corresponds to the forward-modeling voxels. The actual mesoscopic heterogeneity is depicted in the center inversion voxel. The porous material within each fine voxel is implicitly taken to be uniform so that the coefficients of Biot theory apply to the fine voxels.

crosswell application. We assume that mesoscopic heterogeneity is possibly present and so each inversion voxel is further discretized into fine-scaled voxels upon which the forward modeling is to be performed (Figure 8).

To use Biot theory on the fine mesh (the forward model), four material properties must be specified for each of the small voxels: fluid type (if gas and/or oil are possibly present), porosity ϕ, permeability k, and a consolidation parameter c that characterizes how well the framework of grains is cemented together. For example, the drained bulk K_D and shear G_D moduli required in Biot theory can be expressed in an effective-medium-theory form $K_D=K_s(1-\phi)/(1+c\phi)$ and $G_D = G_s(1-\phi)/(1 + 3\ c\phi/2)$, where the solid mineral moduli K_s and G_s are taken as constants.

The four parameters are to be randomly distributed throughout each large inversion voxel using a probability-distribution function (pdf). For example, the porosity ϕ of a fine-scale voxel might be sampled from a Gaussian pdf that is proportional to $\exp(-|(\phi - \langle\phi\rangle|^2/2)$ where the average porosity throughout the inversion voxel is $\langle\phi\rangle$ and the standard of deviation is σ_ϕ. The other fine-scale properties (k and c) are also sampled from similar distributions. There are always questions surrounding which pdf is most appropriate for a given property (the log-normal distribution is often preferred over the normal distribution); however, for our purposes here, the main importance is only that the chosen pdf has both a mean and a variance. Additionally, three correlation lengths ξ_i (i=1,2,3) can be defined for each property in each Cartesian direction i by employing a two-point correlation function of a given form. One possible form is $[\phi(\mathbf{x})\phi(\mathbf{y})] - [\phi(\mathbf{x})][\phi(\mathbf{y})] = |\xi_1/(x_1-y_1)|\,|\xi_2/(x_2-y_2)|\,|\xi_3/(x_3-y_3)|)^m$, where $\mathbf{x}$ and $\mathbf{y}$} are the positions of two fine-scale voxels within an inversion voxel and where angle brackets again denote the average value throughout an inversion voxel. The goal of the inversion, regardless of the forms taken for the pdf and correlation function, is to obtain the mean, variance, and correlation lengths of the three (or four) material properties. There are thus on the order of 10 unknown properties (or more) to determine at each inversion voxel.

Although random properties sampled from a pdf and satisfying a correlation function may not be able to represent every aspect of the actual mesoscopic heterogeneity present, they nonetheless allow for the key effects influencing wave amplitudes: mesoscopic flow between the fine-scale voxels (the likely dominant contribution to intrinsic attenuation); scattering from the mesoscopic and larger scale voxels; and anisotropy through the presence of correlated properties. Also, the particle velocities on the fine-scale grid can be locally averaged to produce synthetic geophone data at the scale that the real geophone groups are measuring the earth response. Such a volume average of the fine response should also make the synthetic seismic data relatively insensitive to the specific realization of the random material properties in each inversion voxel (just how insensitive needs to be numerically tested).

However, the difficulties in attacking this inverse problem using iterative-search methods are many. First, there is the extreme computational cost of forward modeling with such fine discretization (the 3D forward modeling grid would contain at least 1000 times the nodes normally used). Second, analytical expressions must be developed for the Frechét derivatives with respect to the statistical properties. Derivatives with respect to the average properties may not be so difficult; however, the derivatives with respect to correlation length and the variances are not as straightforward. Of course, such Frechét derivatives could be determined numerically but at a very significant cost. Third, the large number (roughly 10) of inversion parameters for each inversion voxel might produce many local minima in the misfit function requiring at least initial use of Monte Carlo global search methods.

Although this inversion approach seems well posed and capable of producing interesting and novel information about the earth from seismic data, it is beyond the ability of present computer power. Tests of the approach on small-scale or 2D models are, however, presently feasible. But application to real-world data sets at real-world scales is not yet numerically possible.

Conclusions and perspectives. This article has explored the question of whether permeability information is present in seismic data. Recent models of loss due to wave-induced flow at mesoscopic scales produce Q values in the seismic band that are similar to what is observed in the field and that directly involve the permeability structure of the material. Thus, it seems likely that seismic amplitudes do contain some type of permeability information.

An inversion strategy was suggested that could, in principle, extract such permeability information from full-waveform three-component data. However, calculations suggest that a typical 3D crosswell application with well spacings as small as even a few tens of meters could require 10 000 Gbytes of dynamic memory which is well beyond present capabilities. In the near term, one could test this inversion strategy by performing laboratory experiments at the scale of meters using controlled materials with known mesoscopic and macroscopic structure. This seems a proper starting point regardless of computer-power constraints.

Also in the near term, the ongoing developments in subtracting scattering attenuation from the measured apparent attenuation must still be encouraged. If such techniques can be improved upon and performed over a wide-enough frequency band without making constant Q assumptions, then again there is hope for extracting permeability information directly from the estimated values of intrinsic attenuation and velocity. Ongoing development of full-waveform inversions that use the entire data set should also be encouraged for these same reasons as should the approach based on downward continuing the prestack seismic data to a targeted interface and performing amplitude versus offset analysis.

Laboratory measurements to help our understanding of the mesoscopic-loss properties at seismic frequencies can conceivably be performed using acoustic-resonance techniques recently developed by Jerry Harris at Stanford University.

In this method, the resonant peaks of an acoustic tank are perturbed by the presence of a rock sample. Depending on the dimensions of the tank and the properties of the fluid filling the tank, the fundamental resonant mode can be made to lie anywhere within the seismic band of frequencies. The shifting and broadening of the tank's resonance peaks due to the presence of the rock sample can be used to estimate the elastic and *Q* properties of the rock within the seismic band. Other laboratory approaches such as using 1-10 kHz piezoelectric transducers on large rock samples (linear dimensions on the order of meters) should also be encouraged.

So in order to obtain permeability information that is likely contained within seismic data, more research is required on: the theoretical nature of forward modeling in porous materials containing mesoscopic heterogeneity; the numerical challenges of using Biot theory on finely discretized grids as the forward model in various inverse schemes; seismic experiments at the meter scale using controlled materials having known mesoscopic and macroscopic heterogeneity; acoustic resonance studies of attenuation in the seismic band; and improving our current abilities to invert for frequency-dependent *Q* from broadband seismic experiments and to subtract the scattering contribution to obtain the intrinsic attenuation. Such an ambitious research agenda has a real chance of resolving the degree to which permeability information can be extracted from seismic data.

Suggested reading. "Inversion of seismic attributes for velocity and attenuation" by Nowack and Matheney (*Geophysical Journal International*, 1997). "Seismic attenuation and tomography using the frequency shift method" by Quan and Harris (GEOPHYSICS, 1997). "The measurement of velocity dispersion and frequency-dependent intrinsic attenuation in sedimentary rocks" by Sams et al. (GEOPHYSICS, 1997). "Scattering and attenuation of seismic waves" by Wu and Aki (three special issues of *Pure and Applied Geophysics* 1988, 1989, and 1990). "Estimation of *Q* from surface seismic reflection data" by Dasgupta and Clark (GEOPHYSICS, 1998). "Reflections on amplitudes" by O'Doherty and Anstey (*Geophysical Prospecting*, 1971). *Seismic Wave Propagation and Scattering in the Heterogeneous Earth* by Sato and Fehler (Springer Verlag & AIP Press, 1998). "Rock mass characterization using intrinsic and scattering attenuation estimates at frequencies from 400 to 1600 Hz" by Feustel et al. (*Pure and Applied Geophysics*, 1996). "A strategy for nonlinear elastic inversion of seismic reflection data" by Tarantola (GEOPHYSICS, 1986). "The state of affairs in inversion of seismic data: An OVSP example" by Charara et al. (SEG 1996 *Expanded Abstracts*). "Target-oriented prestack beamlet migration using Gabor-Daubechies frames" by Chen and Wu (SEG 2002 *Expanded Abstracts*). "Mapping directional illumination and aquisition-aperature efficiency by beamlet propagators" by Wu and Chen (SEG 2002 *Expanded Abstracts*). "Linear dynamics of double-porosity dual-permeability materials" by Pride and Berryman (*Physical Review E*, 2003). "Theory of frequency dependent acoustics in patchy-saturated porous materials" by Johnson (*Journal of the Acoustical Society of America*, 2001). "Theory of propagation of elastic waves in a fluid-saturated porous solid" by Biot (*Journal of the Acoustical Society of America*, 1956). "Squirt flow in fully saturated rocks" by Dvorkin et al. (GEOPHYSICS, 1995). TLE

Acknowledgments: Thanks to Roger Turpening of DOE for the vision and energy to organize a workshop on this theme, and to Marwan Charara of Schlumberger for Figure 4.

Corresponding author: spride@univ-rennes1.fr